PERGAMON

International Journal of Solids and Structures 37 (2000) 669–686

INTERNATIONAL JOURNAL OF SOLIDS and STRUCTURES

www.elsevier.com/locate/ijsolstr

On estimating the tensile strength of an adhesive plastic layer of arbitrary simply connected contour

S. Alexandrov*, O. Richmond

Aluminum Company of America, Alcoa Technical Center, AMCT, Bldg. D, 100 Technical Drive, Alcoa Center, PA 15069-0001, USA

Received 22 September 1998

Abstract

Two approaches for finding three-dimensional kinematically admissible velocity fields in a flat layer of an ideal rigid–plastic material subjected to tension (compression) are proposed. The layer is assumed to have a simply connected but otherwise arbitrary in-plane cross section. The kinematically admissible velocity fields are based on a uniform strain rate field appropriate for a layer without friction and on such a field combined with the asymptotic behavior required of a real velocity field near a velocity discontinuity surface (surface with maximum shear stress). Both of these kinematically admissible velocity fields are used to determine upper bounds on the limit load for layers with quite general yield criteria. Using these limit load solutions, an approach is proposed for estimating the distribution of tensile stresses on the symmetry plane of the layer and, in particular, the value of maximum tensile stress. The latter is of importance for understanding fracture within the layer.

A practical application of this analysis is estimation of the strength of adhesive joints. Numerical calculations are made for an elliptical layer with the Mises yield criterion and for a circular layer with the Tresca yield criterion. The results compare very favorably with available slip line solutions for plane strain and axial symmetry. © 1999 Published by Elsevier Science Ltd. All rights reserved.

Keywords: Strength of joints; Asymptotic behavior; Limit load

1. Introduction

Estimation of the tensile strength of a thin layer of ductile material is of practical interest for the analysis of adhesive joints. When the joining material is much softer than the base material, the latter can be assumed to be rigid. Then the problem reduces to a limit load solution for a thin plastic layer deformed between two rigid bodies. The present paper deals with tension of a thin flat layer with arbitrary in-plane shape. (It is noted, however, that the mathematical formulations of the problems for

* Corresponding author.

PII: S0020-7683(99)00023-2

compression and tension are the same. Therefore, all results for compression of a layer with maximum friction also apply here and vice versa). Since the limit loads for ideal rigid–plastic and ideal elastic–plastic material models coincide (see Drucker et al., 1952), the rigid–plastic model is adopted here. The plane strain compression (tension) of a plastic layer between two rigid plates with maximum friction is a particular case of the problem posed here. The stress solution for this problem was obtained by Prandtl (1923) and the velocity solution by Hill (1950). They used the slip line technique which is restricted to plane strain conditions for the Mises yield criterion but applicable more generally for the Tresca yield criterion. However, some properties of solutions for the ideal rigid–plastic material are common for different yield criteria and for arbitrary deformation. In particular, the asymptotic behavior of the velocity field tangent to velocity discontinuity surfaces and maximum friction surfaces is the same near such surfaces for all investigated yield criteria and modes of deformation. This problem has been investigated by Sokolovskii (1956) for planar flow, by Alexandrov and Druyanov (1992) for axisymmetric flow of Mises material, by Alexandrov (1992, 1995) for arbitrary flow of Mises material, by Alexandrov and Richmond (1998) for axisymmetric flow of Tresca material, and by Alexandrov and Richmond (1997) for three dimensional flow of material obeying general smooth yield criteria. The main result of all of these studies is that the velocity tangent to surfaces with maximum shear stress follows a square root rule near such surfaces.

Alexandrov and Richmond (1997) proposed an approach for evaluating the limit load for the Prandtl problem mentioned above combining the asymptotic velocity field with an appropriate frictionless velocity field. Comparison of this upper bound on the limit load with the slip line solution and solutions obtained by other methods (see, for example Kobayashi and Thomsen, 1964) has shown that the upper bound derived using the new approach lies between those given by the slip line method and the uniform deformation energy method (in the terminology of Kobayashi and Thomsen, 1964). This latter solution for the problem under consideration is simply a solution based on a uniform strain rate field. The difference between the new solution and the slip line solution was very small and compared with that obtained between a finite element solution and experimental results for similar problems (see, for example Kobayashi, 1971). We develop this idea here in order to evaluate the limit load for a plastic layer of arbitrary shape. First, the three-dimensional kinematically admissible velocity field for a frictionless layer of arbitrary shape (spatially uniform strain rates) is given. Then, this velocity field is combined with the required asymptotic velocity field near velocity discontinuity surfaces, which are assumed to exist at the bimaterial interfaces. This leads to a kinematically admissible velocity field which accounts for the behavior of a real velocity field near the velocity discontinuity surfaces and also near the symmetry plane of the layer. Both the uniform strain rate field and the special behavior of the asymptotic field are the same for different yield criteria, so the results given here are quite general.

Distribution of the tensile stress and its maximum value in the layer are of importance for understanding possible fracture in the layer. Using the upper bound theorem alone it is not generally possible to determine such stresses. An extension of the upper bound theorem to include the determination of the local stresses was suggested by Azarkhin and Richmond (1991) who proposed using an iterative numerical procedure after an upper bound solution has been obtained. We propose here an appropriate analytical approach for estimating the tensile stress distribution on the symmetry plane of the layer using the upper bound solution described above. In addition it is assumed, as seen in the known slip line solutions, that there exists a zone near the stress free contour of the layer where the state of stress is uniaxial tension. Moreover, it is assumed that the tensile stress on the symmetry plane of the layer is given by a linear function of an appropriate variable which, generally speaking, should be chosen for each specific shape of the layer. Nevertheless a general approach for a group of shape configurations is proposed. Because of this last assumption the stress distribution is given by nondifferentiable functions, a circumstance that also occurs in slip line solutions under plane strain and axisymmetric conditions. Similar stress distribution have been found in twisted bars by Nadai (1950).

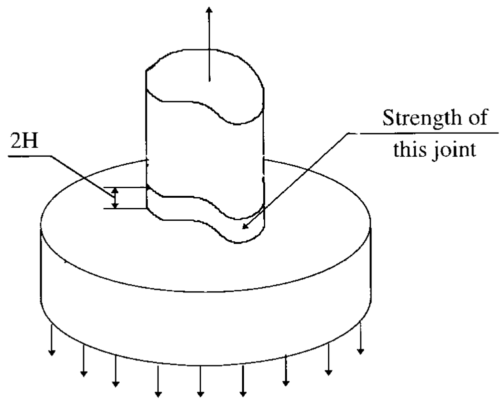

Fig. 1. Illustration of a structure with an adhesive joint.

The calculated limit load gives an estimate of the maximum tensile stress and the tensile stress distribution.

Two numerical examples illustrate the general solutions. Tension of an elliptical layer is considered with the Mises yield criterion. An upper bound load for a circular layer, which is a particular case of the elliptic layer, has been found by Kachanov (1956) and, using the asymptotic velocity field near a surface with maximum friction, by Alexandrov (1994). Axisymmetric tension is also considered for the Tresca yield criterion since it is of special interest for comparison of the proposed approach with a slip line solution obtained by Kwaszczynska and Mroz (1967). Comparison of our solutions with this slip line solution is made for both the limit load and the distribution of tensile stress on the symmetry plane. In addition, the ratio of the maximum tensile stress to the average tensile stress at yielding, which is important for understanding fracture, is analyzed for both examples.

2. Solution with frictionless interface

Let us consider a plastic layer of uniform thickness $2H$ subject to tension between two rigid bodies as shown in Fig. 1. The shape of the layer is arbitrary but is the same in each plane perpendicular to the thickness direction. The contour of the layer is assumed to be stress free. We adopt a Cartesian coordinate system xyz, the z-axis coinciding with the thickness direction and the coordinate surface $z = 0$ coinciding with the symmetry plane of the layer. Then only the space $z \geq 0$ needs to be considered.

In order to find a kinematically admissible velocity field, we assume first that no shear stresses occur on the bimaterial interface. Then we may take the nonzero components of the strain rate tensor to be,

$$-(1+\alpha)\xi_x = -(1+\alpha)\alpha^{-1}\xi_y = \xi_z, \tag{1}$$

where α is a constant, and

$$\xi_z = \frac{v_0}{H}, \tag{2}$$

where v_0 is the velocity of the rigid plate. The range of α is $0 \leq \alpha \leq 1$, since $\alpha < 0$ contradicts the physical sense of the problem and the effect of $\alpha > 1$ can be obtained by interchanging the coordinate axes x and y. It is clear that the strain rates defined by Eq. (1) satisfy the incompressibility condition for any α. Combining Eqs. (1) and (2) with the definitions for strain rate, the velocity field is given by:

$$v_z = \frac{v_0 z}{H}, \quad v_x = -\frac{v_0 x}{H(1+\alpha)} \quad \text{and} \quad v_y = -\frac{v_0 y \alpha}{H(1+\alpha)}. \tag{3}$$

We have chosen the coordinate system such that the layer as a whole does not rotate with respect to the z-axis and the material points on the z-axis move along this axis only. Generally speaking, the coordinate system itself may move but, in the case where no shear stresses occur on the bimaterial interface, such rigid body motions do not influence the solution. However, when this solution is used to determine the limit load for an adhesive interface, shear stresses appear and equilibrium imposes additional restrictions on the specification of the coordinate system.

We mention two cases: $\alpha = 0$, plane strain tension with $\xi_y = 0$; and $\alpha = 1$, axisymmetric tension with $\xi_y = \xi_x$. Using the normality flow rule, the deviatoric portions of the stresses may be found from Eqs. (1) and (2) for any yield criterion independent of the mean stress. It is clear that the components of the stress deviator are constant. If, in addition, we require that the mean stress is uniform then all equilibrium equations are automatically satisfied. Generally, the boundary conditions on the contour of the layer are not satisfied. However, in the special cases, $\alpha = 0$ and $\alpha = 1$, they are satisfied for any smooth yield criterion and, if $\alpha = 1$, for the layer of arbitrary shape. Also, for the Tresca yield criterion the boundary conditions may be satisfied for the layer of arbitrary shape at any α. In these special cases, the mean stress is determined by the boundary conditions and, then, the stress component σ_z determines the exact limit load.

In the case $\alpha = 1$, it will be convenient to use a cylindrical coordinate system, $r\theta z$, with the transformation equations

$$x = r\cos\theta, \quad y = r\sin\theta \quad \text{and} \quad z = z. \tag{4}$$

In these coordinates, the velocity field Eq. (3) at $\alpha = 1$ takes the form

$$v_r = -\frac{v_0 r}{2H}, \quad v_\theta = 0 \quad \text{and} \quad v_z = \frac{v_0 z}{H}. \tag{5}$$

3. Limit load solutions for an adhesive interface

We assume that when the bimaterial interface is adhesive it will be a surface with a velocity discontinuity. Then the absolute value of the shear stresses on this surface will be equal to the shear yield stress, k, analogous to Prandtl's classical problem, and their directions will be opposite to the velocity vectors. Hence,

$$\sigma_{xz} = -k\cos(\mathbf{v}_\tau, \mathbf{i}) \quad \text{and} \quad \sigma_{yz} = -k\cos(\mathbf{v}_\tau, \mathbf{j}) \text{ at } z = H, \tag{6}$$

where $\mathbf{v}_\tau$ is the vector component of the velocity tangent to the bimaterial interface and $\mathbf{i}$ and $\mathbf{j}$ are the base vectors of the Cartesian coordinate system. The velocity field Eq. (3) is still kinematically admissible. Therefore, the simplest way to obtain a limit load is to apply this field. As mentioned before, equilibrium may impose some additional restrictions on the specification of the coordinate system. Thus, we shall satisfy equilibrium for the layer as a whole even though this is not strictly required by the upper bound theorem. It is clear that a coordinate system in which the velocity field is given by Eq. (3)

cannot rotate with respect to the rigid plate which is assumed to move upward without rotation. By definition,

$$\cos(\mathbf{v}_\tau,\mathbf{i}) = \frac{v_x}{\sqrt{v_x^2 + v_y^2}} \quad \text{and} \quad \cos(\mathbf{v}_\tau,\mathbf{j}) = \frac{v_y}{\sqrt{v_x^2 + v_y^2}}. \tag{7}$$

Substituting Eq. (3) into Eq. (7) gives

$$\cos(\mathbf{v}_\tau,\mathbf{i}) = -\frac{x}{\sqrt{x^2 + \alpha^2 y^2}} \quad \text{and} \quad \cos(\mathbf{v}_\tau,\mathbf{j}) = -\frac{\alpha y}{\sqrt{x^2 + \alpha^2 y^2}}. \tag{8}$$

Equilibrium of the layer as a whole requires

$$\int\int_S \sigma_{xy}|_{z=H}\,\mathrm{d}x\,\mathrm{d}y = 0 \quad \text{and} \quad \int\int_S \sigma_{yz}|_{z=H}\,\mathrm{d}x\,\mathrm{d}y = 0, \tag{9}$$

where S is the cross-sectional area. Combining Eqs. (6), (8) and (9), we find for $\alpha \neq 0$

$$\int\int_S \frac{x}{\sqrt{x^2 + \alpha^2 y^2}}\mathrm{d}x\,\mathrm{d}y = 0 \tag{10a}$$

and

$$\int\int_S \frac{y}{\sqrt{x^2 + \alpha^2 y^2}}\mathrm{d}x\,\mathrm{d}y = 0. \tag{10b}$$

If a cross section, z = const, has a symmetry axis then one of the axes of the coordinate system, say y, must coincide with the symmetry axis. In this case, Eq. (10a) vanishes since the integrand is an odd function of x. Analogously, if the cross section has two axes of symmetry, then both axes, x and y, must coincide with these symmetry axes and both integrals (Eqs. (10a) and (10b)) automatically vanish. In the general case, the origin of the coordinate system is determined along with the limit load by minimizing the corresponding functional using the restrictions imposed by Eqs. (10a) and (10b).

In an arbitrary Cartesian coordinate system as defined above, we may write the principle of virtual work rate for the problem under consideration. For an ideal rigid–plastic material obeying the Mises yield criterion, this gives

$$Pv_0 = k\int\int\int_V \sqrt{2\xi_{ij}\xi_{ij}}\,\mathrm{d}V - \int\int_S (v_x\sigma_{xz} + v_y\sigma_{yz})|_{z=H}\,\mathrm{d}S, \tag{11}$$

where P is the limit load and V is the volume of material at $z \geq 0$. Substituting Eqs. (3), (6) and (8) into Eq. (11) then gives the limit load for yielding of the plastic layer based on the frictionless kinematically admissible velocity field Eq. (3). We write the result in the form

$$q_i = \frac{P_i}{kS} = 2\frac{\sqrt{1+\alpha+\alpha^2}}{1+\alpha} + \frac{1}{(1+\alpha)HS}\int\int_S \sqrt{x^2 + \alpha^2 y^2}\,\mathrm{d}x\,\mathrm{d}y. \tag{12}$$

It follows from the upper bound theorem that the best bound is obtained by minimizing q_i with respect to α in this expression.

In order to improve the limit load prediction, we now take into account the known behavior of a real velocity field near an adhesive bimaterial interface which is assumed to be a velocity discontinuity surface. Then the velocity tangent to the surface must follow a square root law (see the references mentioned in the Introduction). We therefore modify the velocity field given by Eq. (3) to the form

$$v_x = -\frac{v_0 x}{H(1+\alpha)}\left(A + B\sqrt{1-\zeta^2}\right) \quad \text{and} \quad v_y = -\frac{v_0 \alpha y}{H(1+\alpha)}\left(A + B\sqrt{1-\zeta^2}\right). \tag{13}$$

where ζ stands for the dimensionless axial coordinate, $\zeta = z/H$, and A and B are constants. We have also taken into account that v_x and v_y are to be even functions of ζ. Combining Eq. (13) and the incompressibility equation, $\partial v_x/\partial x + \partial v_y/\partial y + \partial v_z/\partial z = 0$, gives

$$v_z = v_0\left[A\zeta + \frac{1}{2}B\left(\zeta\sqrt{1-\zeta^2} + \sin^{-1}\zeta\right)\right] + C, \tag{14}$$

where C is a constant of integration. The velocity v_z must satisfy the boundary conditions $v_z = 0$ at $\zeta = 0$ and $v_z = v_0$ at $\zeta = 1$. Therefore $C = 0$ and $A = 1 - \pi B/4$. Then, Eq. (14) takes the form

$$\frac{v_z}{v_0} = \zeta\left[1 - \frac{\pi B}{4} + \left(\frac{B}{2}\right)\sqrt{1-\zeta^2}\right] + \left(\frac{B}{2}\right)\sin^{-1}\zeta \tag{15}$$

and Eq. (13) becomes

$$\frac{v_x}{v_0} = -\frac{x}{H(1+\alpha)}\left(1 - \frac{\pi B}{4} + B\sqrt{1-\zeta^2}\right)$$

and

$$\frac{v_y}{v_0} = -\frac{\alpha y}{H(1+\alpha)}\left(1 - \frac{\pi B}{4} + B\sqrt{1-\zeta^2}\right). \tag{16}$$

It is clear that the velocity field does not influence the equilibrium conditions which we have imposed since the ratio v_y/v_x is the same for the velocity fields given by both Eqs. (3) and (16). Therefore, Eqs. (10a) and (10b) are again restrictions for the specification of the coordinate system. The components of the strain rate tensor are determined from Eqs. (15) and (16) as

$$\xi_x = -\frac{v_0}{H(1+\alpha)}\left(1 - \frac{\pi B}{4} + B\sqrt{1-\zeta^2}\right), \tag{17a}$$

$$\xi_y = -\frac{v_0 \alpha}{H(1+\alpha)}\left(1 - \frac{\pi B}{4} + B\sqrt{1-\zeta^2}\right), \tag{17b}$$

$$\xi_z = \frac{v_0}{H}\left(1 - \frac{\pi B}{4} + B\sqrt{1-\zeta^2}\right), \tag{17c}$$

$$\xi_{xz} = -\frac{v_0 B x \zeta}{2H^2(1+\alpha)\sqrt{1-\zeta^2}}, \tag{17d}$$

$$\xi_{yz} = \frac{v_0 B \alpha y \zeta}{2H^2(1+\alpha)\sqrt{1-\zeta^2}} \tag{17e}$$

and

$$\xi_{xy} = 0. \tag{17f}$$

Eq. (11) is also valid and, with the use of Eqs. (6), (8), (16) and (17a–f) transforms to

$$q_a = \frac{P_a}{kS} = \frac{1}{(1+\alpha)S}\int\int\int_V \sqrt{4(1+\alpha+\alpha^2)\left(1-\frac{\pi B}{4}+B\sqrt{1-\zeta^2}\right)^2 + \frac{B^2\zeta^2}{H^2(1-\zeta^2)}(x^2+\alpha^2y^2)} \times \mathrm{d}x\,\mathrm{d}y\,\mathrm{d}\zeta + \frac{1-\pi B/4}{HS(1+\alpha)}\int\int_S \sqrt{x^2+\alpha^2y^2}\,\mathrm{d}x\,\mathrm{d}y. \tag{18}$$

It follows from the nature of friction forces that the second term in Eq. (18) must be positive at sliding. Therefore,

$$B < \frac{4}{\pi} \tag{19}$$

Moreover, it is clear that $\sigma_{xz} > 0$ and $\sigma_{yz} > 0$ everywhere except on the symmetry plane, so that also $\xi_{xz} > 0$ and $\xi_{yz} > 0$. Then, from Eqs. (17d) and (17e),

$$B > 0. \tag{20}$$

Since, for any layer, the limits of integration with respect to ζ are always from 0 to 1, the volume integral in Eq. (18) is improper. Therefore, we introduce a new variable

$$\chi = \sqrt{1-\zeta}. \tag{21}$$

Finally then, substituting Eq. (21) into Eq. (18) leads to the average yield stress in the form

$$q_a = \frac{P_a}{kS} = \frac{2}{(1+\alpha)S}\int\int\int_V \sqrt{4(1+\alpha+\alpha^2)\left(1-\frac{\pi B}{4}+B\chi\sqrt{2-\chi^2}\right)^2\chi^2 + H^{-2}B^2(2-\chi^2)^{-1}(1-\chi^2)^2(x^2+\alpha^2y^2)} \times \mathrm{d}x\,\mathrm{d}y\,\mathrm{d}\chi + \frac{1-\pi B/4}{HS(1+\alpha)}\int\int_S \sqrt{x^2+\alpha^2y^2}\,\mathrm{d}x\,\mathrm{d}y. \tag{22}$$

The sign of the volume integral has been taken such that the limits of integration with respect to χ are from 0 to 1. Minimization of Eq. (22) with respect to α and B, subject to the bounds on B given by Eqs. (19) and (20), can be carried out numerically to obtain the upper bound for any layer cross section based on the kinematically admissible velocity field (Eqs. (15) and (16)) which accounts for the necessary asymptotic behavior of the velocity field at a velocity discontinuity surface (bimaterial interface).

4. Particular cases: $\alpha = 0$ and $\alpha = 1$

The case $\alpha = 0$ leads to plane strain conditions thus corresponding to the classical Prandtl problem. The solutions based on the approaches developed here have been obtained by Alexandrov and Richmond (1997). The authors have compared their results with a slip line solution and found that the

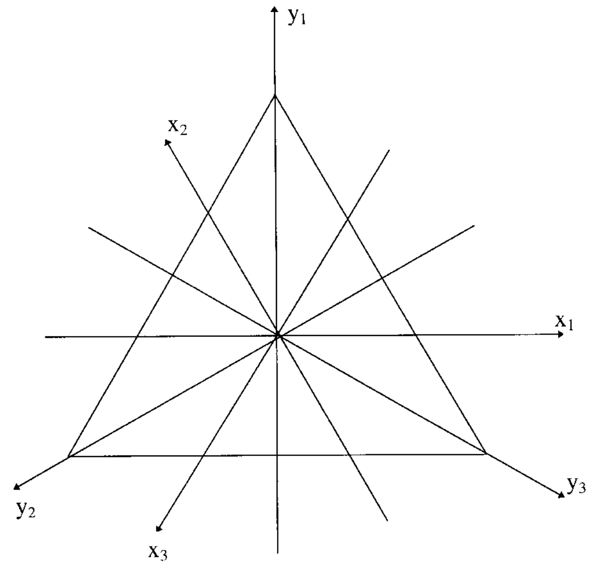

Fig. 2. Cross section in the shape of a regular triangle and equivalent coordinate systems.

relative differences are very small, especially for the solution based on the velocity field accounting for the asymptotic behavior of the velocity field.

The case $\alpha=1$ must be used for some particular cross sections of the layer. In particular, it is clear that $\alpha=1$ for circular and square cross sections because the coordinate system can be chosen such that there will be no difference between the x and y directions. In order to find a totality of cross sections for which $\alpha=1$, we first consider a regular triangle as shown in Fig. 2. It is clear from geometrical considerations that solutions found with the use of each coordinate system shown in Fig. 2 must lead to the same result. In particular, it follows from Eq. (17f) that the directions of the axes x_1, x_2, and x_3 are all principal directions of the strain rate tensor. Since these directions are not orthogonal, this is possible if and only if $\alpha=1$. It is clear that this proof holds for a regular polygon with an arbitrary number of corners, including a circle as the limit case, but excluding a square because, for a square, the corresponding directions are orthogonal. Nevertheless, for square cross sections also, $\alpha=1$ as mentioned above. The main idea of this proof (that there are non orthogonal directions of principal axes of the strain rate tensor or there are two identical principal line directions) can be applied to cross sections of arbitrary shape giving the totality of shapes for which $\alpha=1$. It should be noted that this proof is based on the assumed velocity field and valid only for that case. Indeed, if one allows a more general velocity field it is not necessary that for a regular polygon any direction on the cross section is principal everywhere for the strain rate tensor. On the other hand, calculations are simplified when it is known in advance that $\alpha=1$, giving one less variable to minimize in Eqs. (12) and (22). Therefore, for practical applications, one may take $\alpha=1$ if the cross section under consideration differs little from those for which the condition $\alpha=1$ is strictly required.

At $\alpha=1$, the value of q_i is determined from Eq. (12) by direct calculations without minimization. In this case, it is convenient to adopt the cylindrical coordinate system introduced by Eq. (4). Then Eq. (12) takes the form

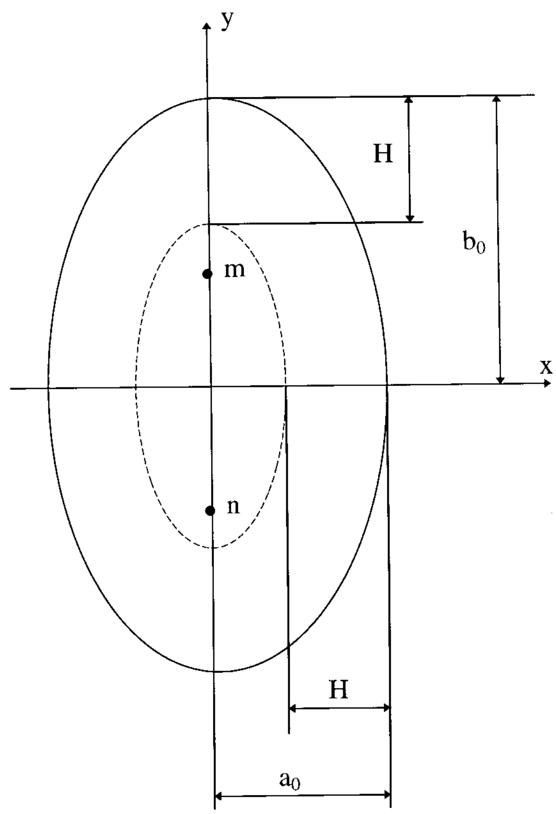

Fig. 3. Elliptical layer. Zones with different analytical expressions for σ_z.

$$q_i = \sqrt{3} + \frac{1}{2HS}\iint_S r^2\,\mathrm{d}r\,\mathrm{d}\theta. \tag{23}$$

The value of q_a follows from Eq. (22):

$$q_a = S^{-1}\iiint_V \sqrt{12\left(1 - \frac{\pi B}{4} + B\chi\sqrt{2-\chi^2}\right)^2 \chi^2 + \frac{B^2(1-\chi^2)^2 r^2}{H^2(2-\chi^2)}}\, r\,\mathrm{d}r\,\mathrm{d}\theta\,\mathrm{d}\chi + \frac{1-\pi B/4}{2HS}\iint_S r^2\,\mathrm{d}r\,\mathrm{d}\theta. \tag{24}$$

In order to obtain the best upper bound, this expression should be minimized with respect to B.

The analysis in Sections 4 and 5 has been explicitly performed for the Mises yield criterion. However, since the asymptotic behavior of the velocity field is the same for quite arbitrary smooth yield criteria (Alexandrov and Richmond, 1997) and for the Tresca yield criterion (Alexandrov and Richmond, 1998), the analysis also holds in these cases. The only difference is that the integrand in the volume integral in Eq. (11) must be taken in the form corresponding to the selected yield criterion.

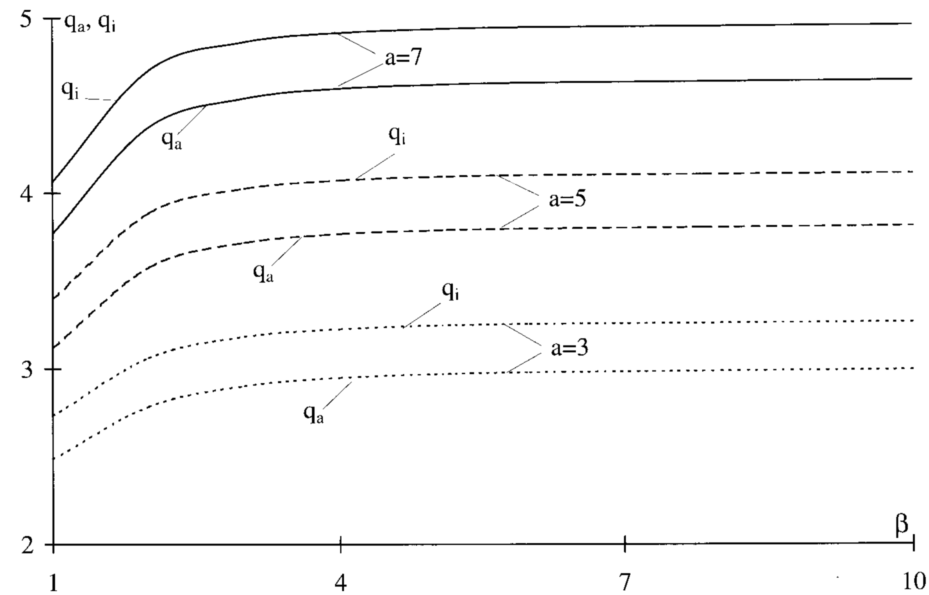

Fig. 4. Variation of the average tensile stress at yielding with the aspect ratio (elliptic cross section, Mises yield criterion).

5. Stress distribution at $z = 0$

Upper bound solutions do not allow one to determine stresses directly. Nevertheless, we propose here a simple analytical approach for approximating the distribution of σ_z on $z = 0$ for possible estimation of fracture limits in the adhesive layer. We assume that the stress distribution corresponding to simple tension is a good approximation to the real stress distribution near the stress free surface of the layer. We also assume that the width of the zone where this distribution occurs is approximately equal to the half thickness of the layer, H. This width is to be defined for each specific problem as illustrated below. Within this zone, any yield criterion gives $\sigma_z = \sigma_Y$, with σ_Y being the tensile yield stress. We mention that these conditions are exactly satisfied for plane strain deformation and for axisymmetric deformation with the Tresca yield criterion. For the same problems, it is well known from slip line solutions that the origin of the coordinate system is a singular point for σ_z, so that its derivatives do not exist at this point. Therefore, it seems that in cases of practical interest with cross sections for which the condition $\alpha = 1$ is satisfied, it is reasonable to assume a linear distribution of σ_z along a radial coordinate. Then σ_z reaches a maximum value, σ_{max}, at the origin of the coordinate system. For such cases, the boundary of the zone where simple tension occurs may be taken to be similar to the contour of the layer but with smaller perimeter. However, it should be noted that, theoretically, it is not always possible to find such a boundary. The maximum value of σ_z is determined using the calculated limit load. In order to assume a stress distribution at $\alpha \neq 1$, it is reasonable to take the σ_z distribution to be similar to the plastic stress function in the cross section of a twisted bar given by Nadai (1950) [pp. 502, 503]. In these cases, the maximum tensile stress is again determined by the limit load.

It seems that for any specific cross section reasonable assumptions may be made to obtain an appropriate stress distribution. Examples will be given in the next section.

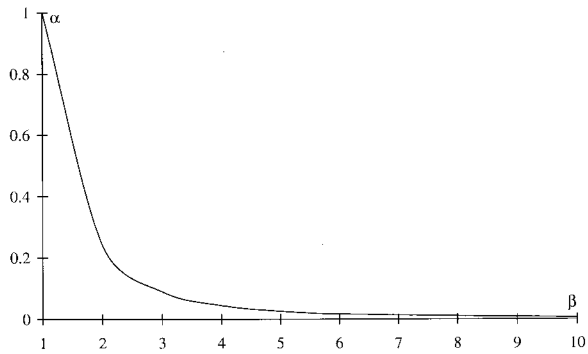

Fig. 5. Variation of α with the aspect ratio (elliptic layer, Mises yield criterion).

6. Examples

6.1. Elliptical layer, $\alpha \neq 1$

Let a_0 and b_0 be the half lengths of the principal axes of an ellipse. Since a cross section, z = const, has two axes of symmetry, the axes of the Cartesian coordinate system should coincide with these axes. Then, Eqs. (10a) and (10b) are automatically satisfied. An arbitrary cross section, z = const, is shown in Fig. 3. Let us introduce the dimensionless coordinates, $X = x/a_0$ and $Y = y/b_0$, and the half length of the axes, $a = a_0/H$ and $b = b_0/H$. The equation of the ellipse in the Cartesian coordinate system may then be written in the form

$$X^2 + Y^2 = 1 \tag{25}$$

and the area of the cross section as

$$S = \pi abH^2. \tag{26}$$

Using Eqs. (25) and (26), Eq. (12) may be transformed to

$$q_i = \frac{\sqrt{1+\alpha+\alpha^2}}{1+\alpha} + \frac{4a}{\pi(1+\alpha)}\int_0^1 \int_0^{\sqrt{1-X^2}} \sqrt{X^2 + \alpha^2\beta^2 Y^2}\,\mathrm{d}Y\,\mathrm{d}X, \tag{27}$$

where β is the aspect ratio, $\beta = b_0/a_0$. Minimization of this expression with respect to α has been carried out numerically. The variation of q_i with β for different values of a is shown in Fig. 4. The limit load for a circular cross section is determined at $\beta = 1$ where $\alpha = 1$. The dependence of α on β is nearly the same for all considered values of a and is shown in Fig. 5. One can see from this figure that, as the aspect ratio β increases, the value of α decreases, very quickly approaching the plane strain value at $\beta \to \infty$. Analogously, we may obtain the expression for q_a from Eq. (22) in the form

$$q_a = \frac{8}{\pi(1+\alpha)}\int_0^1\int_0^1\int_0^{\sqrt{1-X^2}} \sqrt{4(1+\alpha+\alpha^2)\left(1-\frac{\pi B}{4}+B\chi\sqrt{2-\chi^2}\right)^2\chi^2 + a^2B^2(2-\chi^2)^{-1}(1-\chi^2)^2(X^2+\alpha^2\beta^2Y^2)} \times \mathrm{d}Y\,\mathrm{d}X\,\mathrm{d}\chi + \frac{4a(1-\pi B/4)}{\pi(1+\alpha)}\int_0^1\int_0^{\sqrt{1-\chi^2}}\sqrt{X^2+\alpha^2\beta^2Y^2}\,\mathrm{d}X\,\mathrm{d}Y. \tag{28}$$

This expression has been minimized numerically with respect to B and α. Variation of q_a with β for different values of a is shown in Fig. 4. One can see from this figure that $q_a < q_i$ at any a and β because the kinematically admissible velocity field for q_a fulfills an added requirement of the actual velocity field. The α value differs very little from that given in Fig. 5. The B value satisfies the conditions of Eqs. (19) and (20).

In order to find a distribution of the σ_z stress and its maximum value, we assume that the boundary of the zone where $\sigma_z = \sigma_Y$ is also an ellipse with the equation

$$\frac{x^2}{(a_0-H)^2} + \frac{y^2}{(b_0-H)^2} = 1. \tag{29}$$

We also assume that the stress σ_z is singular on the line mn between the foci of the ellipse given by Eq. (29). The cross section divided into the zones with different analytical expressions for σ_z and the mn line are shown in Fig. 3. For the problem under consideration, it is natural to adopt an elliptic–hyperbolic coordinate system with the transformation equations (see, for example Flugge, 1972; p. 194)

$$x = z_0 \sinh\lambda \sin\mu \tag{30a}$$

and

$$y = z_0 \cosh\lambda \cos\mu. \tag{30b}$$

The multiplier z_0 has been introduced to satisfy the condition that a coordinate line $\lambda = \lambda_0$ coincides with the curve given by Eq. (29) which is, of course, an additional assumption. (We have also interchanged the notation of the axes used by Flugge, 1972). Then,

$$z_0 = H\sqrt{(b-1)-(a-1)^2}$$

and

$$\tanh\lambda_0 = \frac{a-1}{b-1}. \tag{31}$$

It is clear from Eq. (30a) that the value of z_0 gives the half length of the mn line. As proposed in Section 5, the stress σ_z should satisfy the conditions $\sigma_z = \sigma_Y$ at $\lambda = \lambda_0$ and $\sigma_z = \sigma_{\max}$ at $\lambda = 0$. The simplest way to satisfy both of these conditions is to assume

$$\sigma_z = [\sigma_{\max}(\lambda_0 - \lambda) + \sigma_Y\lambda]\lambda_0^{-1}. \tag{32}$$

The area element in an elliptic–hyperbolic coordinate system is given by

$$\mathrm{d}S = H^2[(b-1)^2 - (a-1)^2](\cosh^2\lambda - \cos^2\mu)\mathrm{d}\lambda\,\mathrm{d}\mu. \tag{33}$$

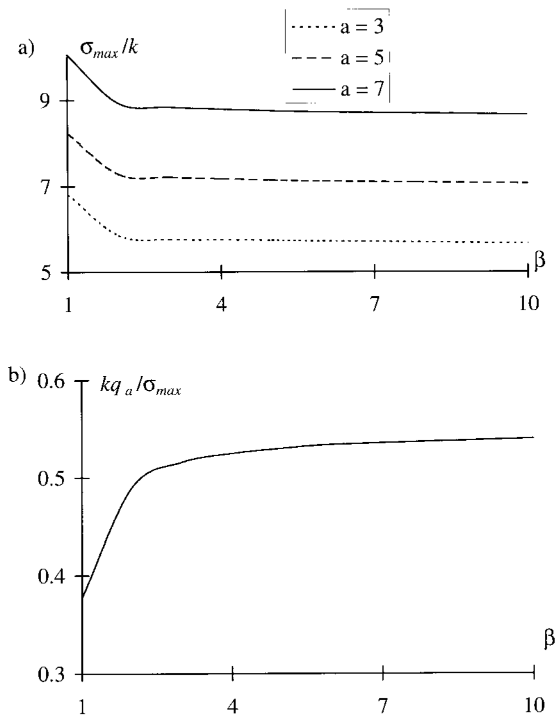

Fig. 6. Variation of the maximum tensile stress and the ratio of the average tensile stress to the maximum tensile stress with the sizes of the layer.

The limit load may be expressed as

$$\frac{P}{4} = \frac{\sigma_Y S_0}{4} + \int_0^{\frac{\pi}{2}} \int_0^{\lambda_0} \sigma_z \, dS, \tag{34}$$

where S_0 is the area of the zone where $\sigma_z = \sigma_Y$. It follows from Eqs. (26) and (29) that

$$S_0 = \pi H^2 (b + a - 1). \tag{35}$$

The value P in Eq. (34) may be replaced by P_i or P_a. Then this equation determines $\sigma_{\max}$ and, with the use of Eq. (32), the distribution of the stress σ_z at $z = 0$. Since $\sigma_Y = \sqrt{3}k$ for the Mises yield criterion, substituting Eqs. (32), (33) and (35) into Eq. (34) gives

$$\frac{\sigma_{\max}}{k} = \frac{\left\{ \dfrac{[qab - \sqrt{3}(b + a - 1)]\pi\lambda_0}{4[(b-1)^2 - (a-1)^2]} - \sqrt{3} \displaystyle\int_0^{\frac{\pi}{2}} \int_0^{\lambda_0} \lambda(\cosh^2\lambda - \cos^2\mu) d\lambda \, d\mu \right\}}{\displaystyle\int_0^{\frac{\pi}{2}} \int_0^{\lambda_0} (\lambda_0 - \lambda)(\cosh^2\lambda - \cos^2\mu) d\lambda \, d\mu}. \tag{36}$$

The value of $\sigma_{\max}/k$ has been calculated using $q = q_a$ giving the results shown in Fig. 6(a). The ratio

$kq_a/\sigma_{\max}$, which is important for evaluating fracture, is nearly the same for all considered values of a and its dependence on β is shown in Fig. 6(b).

As $\beta \to \infty$, the results should be close to those obtained for Prandtl's classical solution. Hill (1950) gives the following equation approximating the results of a slip line solution for $a \geq 1$

$$q_{\Pr} = \frac{(3+a)}{2}$$

in our nomenclature ($2a$ should be considered as the width of the plate). Applying the approach proposed in Section 5, one may obtain

$$\frac{\sigma_{\max}}{k} = 5.5;\ 7.4 \text{ and } 9.4 \text{ at } a = 3;\ 5 \text{ and } 7,$$

respectively and $q_{\Pr}k/\sigma_{\max}$ is approximately 0.54 for these values of a. It is seen from Fig. 6 that these results are in agreement with our calculations for large β.

6.2. Axisymmetric layer, $\alpha = 1$

Tension of an axisymmetric layer for the Tresca yield criterion is of special interest for verification of the proposed approaches since a slip line solution for this case has been obtained by Kwaszczynska and Mroz (1967). These researchers investigated compression but this does not matter as mentioned previously. In the case of the Tresca yield criterion, Eq. (11) should be replaced by

$$Pv_0 = 2k\iiint_V |\xi_{\max}|\,\mathrm{d}V - \iint_S (v_r\sigma_{rz})|_{z=H}\,\mathrm{d}s, \tag{37}$$

where $\xi_{\max}$ is the principal strain rate of maximum absolute value.

Let R_0 be the radius of the layer. In order to apply the first approach, we take the velocity field Eq. (5) as kinematically admissible. It is clear that, in this case,

$$|\xi_{\max}| = \xi_z = \frac{v_0}{H}. \tag{38}$$

The surface integral in Eq. (37) coincides with that of Eq. (11). Therefore, combining Eqs. (37) and (38) we find an upper bound in the form

$$q_i = 2 + \frac{\pi R_0^3}{(3HS)}. \tag{39}$$

Since, for the round layer

$$S = \pi R_0^2, \tag{40}$$

Eq. (39) results in

$$q_i = 2 + \frac{r_0}{3}. \tag{41}$$

with $r_0 = R_0/H$.

In order to obtain an improved upper bound based on the asymptotic velocity field, we may also use the velocity field given by Eqs. (15) and (16) with $\alpha = 1$. Because of symmetry, the circumferential strain rate is a principal one and can be found from Eq. (16) as

$$\xi_\theta = -\frac{v_0}{2H}\left(1 - \frac{\pi B}{4} + B\sqrt{1-\zeta^2}\right). \tag{42}$$

The principal strain rates in a meridian plane are given by

$$\xi_{1,2} = \frac{1}{2}(\xi_r + \xi_z) \pm \frac{1}{2}\sqrt{(\xi_r - \xi_z)^2 + 4\xi_{rz}^2}. \tag{43}$$

Using Eqs. (15), (16) and (42), we can rewrite Eq. (43) in the form

$$\xi_{1,2} = -\frac{1}{2}\left(\xi_\theta \mp \sqrt{9\xi_\theta^2 + 4\xi_{rz}^2}\right). \tag{44}$$

It is clear from this equation that the principal strain rate of the maximum absolute value lies in a meridian plane. Since $\xi_\theta < 0$, we have $\xi_r + \xi_z > 0$, and then it follows from Eq. (44) that

$$|\xi_{\max}| = \frac{1}{2}\left(-\xi_\theta + \sqrt{9\xi_\theta^2 + 4\xi_{rz}^2}\right). \tag{45}$$

The shear strain rate may be calculated from the velocity field, and then substituted together with Eq. (42) into Eq. (45) to give,

$$|\xi_{\max}| = \frac{v_0}{4H}\left[1 - \frac{\pi B}{4} + B\sqrt{1-\zeta^2} + \sqrt{9\left(1 - \frac{\pi B}{4} + B\sqrt{1-\zeta^2}\right)^2 + \frac{\rho^2 B^2 \zeta^2}{1-\zeta^2}}\right]. \tag{46}$$

The surface integral in Eq. (37) coincides with that in Eq. (11). Therefore, substituting Eq. (46) into Eq. (37) and taking into account the axial symmetry of the problem leads to

$$q_a = 2r_0^{-2}\int_0^1\int_0^{r_0}\left[1 - \frac{\pi B}{4} + B\sqrt{1-\zeta^2} + \sqrt{9\left(1 - \frac{\pi B}{4} + B\sqrt{1-\zeta^2}\right)^2 + \frac{\rho^2 B^2 \zeta^2}{1-\zeta^2}}\right]\rho\,\mathrm{d}\rho\,\mathrm{d}\zeta + \frac{r_0}{3}\left(1 - \frac{\pi B}{4}\right).$$

Using Eq. (21), this equation may be transformed into

$$q_a = r_0^{-2}\int_0^1\int_0^{r_0}\left[\left(1 - \frac{\pi B}{4} + B\chi\sqrt{2-\chi^2}\right)\chi + 9\left(1 - \frac{\pi B}{4} + B\chi\sqrt{1-\chi^2}\right)^2\chi^2 + \frac{\rho^2 B^2(1-\chi^2)}{2-\chi^2}\right]$$
$$\times\,\rho\,\mathrm{d}\rho\,\mathrm{d}\chi + \frac{r_0}{3}\left(1 - \frac{\pi B}{4}\right).$$

The upper bound has been found numerically minimizing this expression for q_a with respect to B. Dependence of q_a on r_0 is given quite accurately by a linear function

$$q_a = 1.79 + 0.33r_0. \tag{47}$$

Kwaszczynska and Mroz (1967) have determined an upper bound numerically using the slip line technique. We refer to their results for $r_0 = 3$ after Szczepinski (1979) [p. 235]. Kwaszczynska and Mroz found $q_{\mathrm{KM}} = 2.72$. Our results for this value of r_0 are $q_i = 3$ and $q_a = 2.78$. Thus, the relative differences between the slip line solution and our solutions, especially that based on the asymptotic velocity field, are very small.

In order to determine the stress distribution we adopt here the approach proposed in Section 5 for cross sections with $\alpha = 1$. The σ_z stress distribution is assumed to be

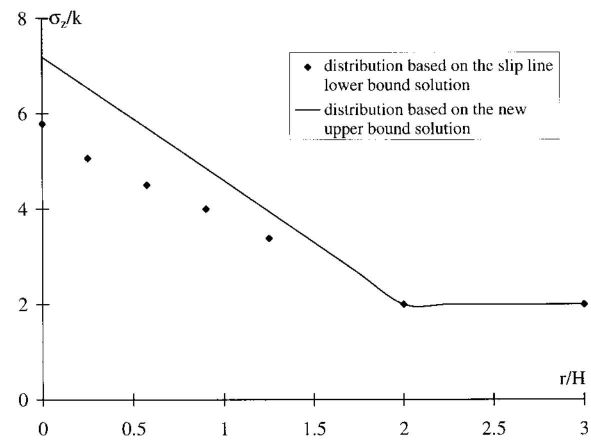

Fig. 7. Distribution of tensile stresses on the symmetry plane of a circular layer based on the slip line lower bound solution and new upper bound solution for $r_0=3$.

$$\sigma_z = \frac{[\sigma_{\max}(R_0 - H - r) + \sigma_Y r]}{(R_0 - H)} \tag{48}$$

at $0 \le r \le R_0 - H$. Then the limit load is given by

$$P = \sigma_Y \pi H(2R_0 - H) + \frac{2}{3}\pi(R_0 - H)^2\left(\frac{\sigma_{\max}}{2} + \sigma_Y\right). \tag{49}$$

Taking into account that $\sigma_Y = 2k$ for the Tresca yield criterion, we find $\sigma_{\max}$ from Eq. (49)

$$\frac{\sigma_{\max}}{k} = \frac{3\left(qr_0^2 - 4r_0 + 2\right)}{(r_0 - 1)^2} - 4. \tag{50}$$

Calculations have been made putting $q = q_a$. The ratio $kq_a/\sigma_{\max}$ is approximately constant within the considered range of r_0 and is between 0.38 and 0.4. The distribution of σ_z along the radius based on the lower bound slip line solution of Kwaszczynska and Mroz along with our results based on the upper bound solution are given for $r_0 = 3$ in Fig. 7.

7. Concluding remarks

An approach for estimating the yield load for plastic layers of uniform thickness and arbitrary in-plane simple connected shape has been proposed. Kinematically admissible velocity fields are based on an appropriate velocity field for a frictionless layer and the known asymptotic behavior of the real velocity field near the bimaterial interfaces in a layer with a velocity discontinuity at these surfaces. Specific expressions in integral form have been obtained for the tensile or compressive yield load, but the approach can be applied to other deformation modes such as bending, torsion and combinations of these with normal loading. In the most general form, the calculations of the limit load require minimization with respect to two variables. However, it has been shown that there is a group of cross sections of practical interest for which this number can be reduced to one. In addition to the necessary requirements of the upper bound theorem, overall equilibrium of the layer is satisfied in all solutions.

A possible application of these solutions is the estimation of the strength of adhesive joints. For this purpose, not only the limit load, but also the maximum tensile stress in the layer is of importance. To this end a simple analytical approach using the calculated limit load has been proposed to determine the distribution of the tensile stress on the symmetry plane of the layer, including the maximum tensile stress. It has been assumed that the σ_z stress is singular at some point or on some line. In the example it was natural to adopt an elliptic–hyperbolic coordinate system which formed such a line. In more general cases it seems that the medial axis of a cross section might be used as a singular line for the stress. For brittle material and for very thin layers, fracture may occur at a lower load than the limit load. In such situations the approach can show that an analysis of brittle fracture must be added.

The general analysis holds for quite arbitrary yield criteria independent of the mean stress. Numerical examples have been given for the Mises and Tresca yield criteria. Tension of an elliptical layer has been investigated for the Mises yield criterion and tension of a circular layer, for the Tresca yield criterion. The results of the latter case have been compared with a known slip line solution for this problem illustrating good agreement for both the limit load and the tensile stress distribution.

The general approach used here for simply connected joints can be extended to multiply connected joints such as are needed for joining hollow sections. However, in this case, the underlying frictionless velocity field must be modified. This will be the subject of a subsequent investigation.

References

Alexandrov, S.E., 1992. Discontinuous velocity fields due to arbitrary strains in an ideal rigid–plastic body. Sov. Phys. Dokl. 37 (6), 283–284 (Trans. from Russian).

Alexandrov, S.E., 1994. Upper bound for the force in upsetting a cylinder with rigid plates. Izv. RAN MTT (Mechanics of Solids) 29 (5), 84–89 (Trans. from Russian).

Alexandrov, S.E., 1995. Velocity field near its discontinuity in an arbitrary flow of an ideal rigid–plastic material. Izv. RAN MTT (Mechanics of Solids) 30 (5), 111–117 (Trans. from Russian).

Alexandrov, S.E., Druyanov, B.A., 1992. Friction conditions for plastic bodies. Izv. AN SSSR MTT (Mechanics of Solids) 27 (4), 110–115 (Trans. from Russian).

Alexandrov, S., Richmond, O., 1997. Asymptotic Plastic Flow Fields Near Surfaces of Maximum Friction Stress. Alcoa Technical Report.

Alexandrov, S.E., Richmond, O., 1998. Asymptotic behavior of the velocity field near surfaces with maximum friction for axisymmetric plastic flow of Tresca material. Dokl. Rus. Acad. Sci. 360 (4), 480–482 (in Russian).

Azarkhin, A., Richmond, O., 1991. Extension of the upper bound method to include estimation of stresses. J. Appl. Mech. 58, 493–498.

Drucker, D.C., Prager, W., Greenberg, H.J., 1952. Extended limit design theorems for continuous media. Quart. Appl. Math. 9, 381–389.

Flugge, W., 1972. Tensor Analysis and Continuum Mechanics. Springer–Verlag, Berlin.

Hill, R., 1950. The Mathematical Theory of Plasticity. Clarendon Press, Oxford.

Kachanov, L.M., 1956. Foundations of Plasticity Theory. GITTL, Moscow (in Russian).

Kobayashi, S., Thomsen, E.G., 1964. Methods of solution of metal-forming problems. In: Backofen, W.A., Burke, J.J., Coffin, L.F.Jr., Reed, N.L., Weiss, V. (Eds.), Fundamentals of Deformation Processing, Proc. 9th Sagamore Army Materials Research Conf. Syracuse University Press, Syracuse, pp. 43–69.

Kobayashi, S., 1971. Theories and experiments on friction, deformation, and fracture in plastic deformation processes. In: Hoffmanner, A.L. (Ed.), Metal Forming: Interrelation Between Theory and Practice. Plenum Press, New York and London, pp. 325–347.

Kwaszczynska, K., Mroz, Z., 1967. A theoretical analysis of plastic compression of short circular cylinders. Arch. Mech. Stos. 19, 787–797.

Nadai, A., 1950. Theory of Flow and Fracture of Solids. McGraw–Hill, New York.

Prandtl, L., 1923. Anwendungsbeispiele Zu Einem Henckyschen Satz Uber Das Plastische Gleichgewicht. Zeitschr. Angew. Math. Mech. 3, 401–406.
Sokolovskii, V.V., 1956. Equations of plastic flow in a surface layer. Prikladnay Matematika i Mechanicka (PMM) 20, 328–334 (in Russian).
Szczepinski, W., 1979. Introduction to the Mechanics of Plastic Forming of Metals. Sijthoff & Noordhoff, Alphen aan den Rijn.